Steel and Composite Structures, *Vol. 22, No. 6 (2016) 1445-1463*
DOI: http://dx.doi.org/10.12989/scs.2016.22.6.1445

Hygrothermal effects on buckling of composite shell-experimental and FEM results

Madhusmita Biswal [1], Shishir Kr. Sahu [*2], A.V. Asha [2] and Namita Nanda [3]

[1] *School of Civil Engineering KIIT University, Bhubaneswar, Odisha 751024, India*
[2] *Department of Civil Engineering National Institute of Technology, Rourkela, Odisha 769008, India*
[3] *Department of Applied Mechanics, Indian Institute of Technology, Delhi 110016, India*

(*Received May 23, 2016, Revised November 28, 2016, Accepted December 01, 2016*)

Abstract. The effects of moisture and temperature on buckling of laminated composite cylindrical shell panels are investigated both numerically and experimentally. A quadratic isoparametric eight-noded shell element is used in the present analysis. First order shear deformation theory is used in the present finite element formulation for buckling analysis of shell panels subjected to hygrothermal loading. A program is developed using MATLAB for parametric study on the buckling of shell panels under hygrothermal field. Benchmark results on the critical loads of hygrothermally treated woven fiber glass/epoxy laminated composite cylindrical shell panels are obtained experimentally by using universal testing machine INSTRON 8862. The effects of curvature, lamination sequences, number of layers and aspect ratios on buckling of laminated composite cylindrical curved panels subjected to hygrothermal loading are considered. The results are presented showing the reduction in buckling load of laminated composite shells with the increase in temperature and moisture concentrations.

Keywords: hygrothermal effects; buckling; woven fiber; Glass/Epoxy; laminated cylindrical shell panels; FSDT; FEM

1. Introduction

Shells of laminated composite materials are becoming increasingly used in aircraft fuselage, spacecraft, rockets, cars, ballistic missiles, submarine hulls, boats, storage tanks and the roofs of buildings because of their high specific strength, stiffness, low specific density, tailorability in challenging applications, excellent thermal characteristics and simplicity in fabrication. The predominant force acting in shells erected in an aircraft or spacecraft structure is axial compression which causes buckling. Thin laminated composites shell structures might buckle before they reach the strength limit. The Ariane 5 launcher (Agency 2012) is an example of an application of cylindrical shell prone to buckling due to compressive loading. The static stability or buckling of structures especially composite curved panels is an important field of research associated with the optimum design of systems. Since the buckling of an engineering structure may lead to collapse of structure, the primarily concern in many applications is the stability of the structure, and both experimental and numerical solution is necessary to predict the critical buckling load. These

*Corresponding author, Professor, E-mail: sksahu.nitrkl@gmail.com

http://www.techno-press.org/?journal=scs&subpage=6 ISSN: 1229-9367 (Print), 1598-6233 (Online)

structures are encountered with considerable variation in environmental conditions including temperature and moisture variations during their service life. The buckling behaviour of laminated composite shell structures are significantly affected by the varying environmental conditions due to moisture absorption and temperature. Therefore the accurate analysis of the buckling response of the laminated composite shell structures under hygrothermal loading are of great practical significance in the prediction of structural behavior of these types of structures.

A number of researches have been carried out on the buckling of laminated composite shells without considering the effects of temperature and moisture absorption. The literature on buckling of moderately thick laminated composite shells is reviewed by Simitses (1996) through 1996. Buckling behavior of laminated composite cylindrical panels under axial compression was studied by Jun and Hong (1988) using finite element method (FEM).The buckling of cross-ply circular cylindrical shells were presented by Khdeir *et al*. (1989) using various shell theories. The effects of shear deformation and curvature on buckling and vibrations of cross-ply laminated composite doubly curved shells were investigated by Carrera (1991) using exact solutions. Nosier and Reddy (1992) analyzed the buckling of cross-ply laminated circular cylindrical shells using Donnell's classical theory. Kim (1996) analysed the buckling of laminated plates and shells under axial compression by using FEM. Matsunaga (1999) studied the buckling of thick shallow shell subjected to in-plane stresses using higher order shallow shell theory. The buckling behaviour of composite shells was studied by Ferreira and Barbosa (2000) using FEM. The buckling of laminate composite shells subjected to transverse load was studied by Sairam and Babu (2002) using FEM based on higher order shear deformation theory. The nonlinear post buckling analysis of laminated composite doubly curved shells was carried out by Kundu and Sinha (2007) utilizing FEM based on virtual work principle. Jung and Han (2014) investigated the shear buckling responses of laminated composite shells using FEM based on FSDT. The buckling behaviour of advanced grid stiffened structure was investigated by Ren *et al*. (2014) using finite element model.

Vibration and buckling of exponentially graded material sandwich plate resting on elastic foundations under various boundary conditions was presented by Meziane *et al*. (2014) using refined shear deformation theory. Belabed *et al*. (2014) investigated bending and vibration of functionally graded plates using higher order shear deformation theory. Hebali *et al*. (2014) studied the bending and vibration analysis of functionally graded plates by using quasi-three-dimensional hyperbolic shear deformation theory. Bending and vibration of functionally graded beams was investigated by Bourada *et al*. (2015) using a refined trigonometric higher order beam theory. Bending and free vibration analysis of isotropic, functionally graded, sandwich and laminated composite plates was investigated by Mahi *et al*. (2015) using hyperbolic shear deformation theory. Higher-order shear deformation plate theory was used by Yahia *et al*. (2015) to study wave propagation in functionally graded plates. Bending and dynamic behaviors of functionally graded plates was studied by Bellifa *et al*. (2016) using FSDT. The free vibration analysis of functionally graded sandwich plates was presented by Bennoun *et al*. (2016) using a five-variable refined plate theory. Vibration and buckling analyses of laminated panels with and without cut-outs under compressive and tensile edge loads was done by Rajanna *et al*. (2016) using FEM.

Study on the buckling of laminated composite shells subjected to hygrothermal environment is much less in the literature. Hygrothermal effects on the stability of a general orthotropic cylindrical composite shell panel subjected to axial or in-plane shear loading was investigated by Lee and Yen (1989) using FEM. Thangaratnam *et al*. (1990) used FEM for linear buckling analysis cof laminated composite cylindrical and conical shells under thermal loading. Hygrothermal effects on the post-buckling of composite laminated cylindrical shell panels were studied by Shen

(2000) using analytical model. Buckling analysis of laminated cylindrical composite shell panel under mechanical and hygrothermal loads was done by Thinh and Ngoc (2005) using FEM. The effect of thermal load on vibration, buckling and dynamic stability of functionally graded cylindrical shells embedded in an elastic medium was studied by Sheng and Wang (2008) using (FSDT).Thermal buckling analysis of laminated conical shell embedded with and without piezoelectric layer subjected to uniform temperature rise was investigated by Singh and Babu (2009) using FEM based on higher order shear deformation theory (HSDT). The effect of random system properties on the post buckling load of geometrically nonlinear laminated composite cylindrical shell panel subjected to hygrothermomechanical loading was dealt by Lal *et al*. (2011) using HSDT.

The thermo-mechanical bending response of functionally graded plates resting on Winkler-Pasternak elastic foundation was studied by Bouderba *et al*. (2013) using refined trigonometric shear deformation theory. Tounsi *et al*. (2013) presented the thermo-elastic bending analysis of functionally graded sandwich plates by utilizing refined trigonometric shear deformation theory. FSDT was used by Bouderba *et al*. (2016) for thermal buckling analysis of functionally graded sandwich plates with various boundary conditions. The bending response of functionally graded plate resting on elastic foundation and subjected to hygro-thermo-mechanical loading was studied by Zidi *et al*. (2014) Using refined plate theory. The thermo-mechanical bending analysis of functionally graded sandwich plates was presented by Hamidi *et al*. (2015) using sinusoidal plate theory. Buckling and post-buckling of anisotropic laminated cylindrical shells under combined external pressure and axial compression in thermal environments were studied by Li and Qiao (2015) using boundary layer theory. Bending behaviour of laminated composite flat panel under hygro-thermo-mechanical loading was presented by Kar *et al*. (2015) using HSDT. Finite difference method was used by Bouguenina *et al*. (2015) to investigate the thermal buckling of simply supported FGM plate with variable thickness.

A critical review of literature on buckling of shells indicate that many studies are appeared in the literature on buckling of laminated shells in ambient conditions using various analytical and numerical approaches. The studies on the buckling of laminated composite shells subjected to hygrothermal environment are limited in the literature. To the best of the author's knowledge, there is no literature dealing with the experimental work on the buckling of woven fabric laminated composite shell panels subjected to variations of temperature and moisture. Experimental studies give the real picture about behaviour of the structure under these conditions. The present study deals with the buckling of bidirectional glass/epoxy composite cylindrical shell panels in hygrothermal environment experimentally for the first time. The authors also developed a code in MATLAB environment for comparing the experimental results using finite element method (FEM).

2. The basic problem

Fig. 1 shows a laminated cylindrical curved panel of length 'a' width 'b' and constant thickness 'h', having 'n' number of thin laminae, every one of which can be oriented at an angle θ with reference to the x-axis of the co-ordinate system. Details of laminated cylindrical curved panel layers are shown in Fig. 2. In the present study, the FSDT has been employed to study the hygrothermal buckling response of a laminated composite shell subjected to uniform temperature and moisture rise. The displacement vector for the model is

$$\{q\} = \{u \;\; v \;\; w \;\; \theta_x \;\; \theta_y\}^T \tag{1}$$

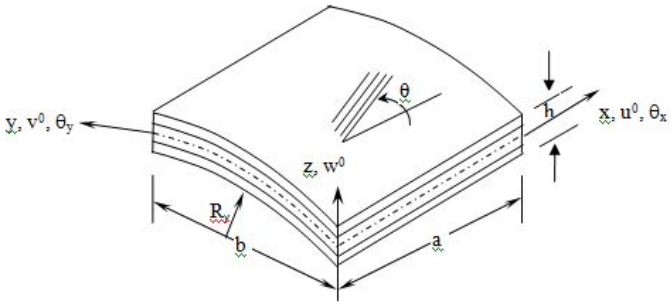

Fig. 1 Cylindrical composite shell configuration

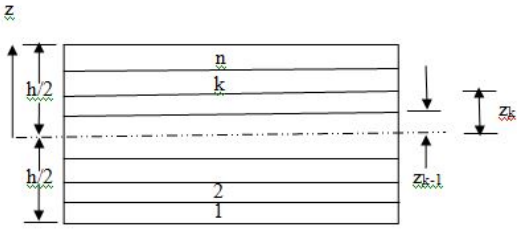

Fig. 2 Details of layer

2.1 Strain displacement relations

Green-Lagrange's strain displacement relations presented by Hsu *et al*. (1981) are used for the structural analysis. The linear part of the strain is used to derive the elastic stiffness matrix. The non-linear part of the strain is used to derive the geometric stiffness matrix and initial stress stiffness matrix due to hygrothermal loading

$$\{\varepsilon\} = \{\varepsilon_l\} + \{\varepsilon_{nl}\} \tag{2}$$

The linear strains corresponding to the displacement given by Eq. (1) is expressed as

$$\varepsilon_{xl} = \frac{\partial u}{\partial x} + zk_x, \qquad \varepsilon_{yl} = \frac{\partial v}{\partial y} + \frac{w}{R_y} + zk_y, \qquad \gamma_{xyl} = \frac{\partial u}{\partial y} + \frac{\partial v}{\partial x} + zk_{xy}$$
$$\gamma_{xzl} = \frac{\partial w}{\partial x} + \theta_x, \qquad \gamma_{yzl} = \frac{\partial w}{\partial y} + \theta_y - C_1 \frac{v}{R_y} \tag{3}$$

where the bending strains k_j are expressed as

$$k_x = \frac{\partial \theta_x}{\partial x}, \qquad k_y = \frac{\partial \theta_y}{\partial y}$$
$$k_{xy} = \frac{\partial \theta_x}{\partial y} + \frac{\partial \theta_y}{\partial x} + \frac{1}{2} C_2 \left(\frac{1}{R_y} \right) \left(\frac{\partial v}{\partial x} - \frac{\partial u}{\partial y} \right) \tag{4}$$

The non-linear strain components are

$$\varepsilon_{xnl}=\frac{1}{2}\left(\frac{\partial u}{\partial x}\right)^2+\frac{1}{2}\left(\frac{\partial v}{\partial x}\right)^2+\frac{1}{2}\left(\frac{\partial w}{\partial x}\right)^2+\frac{1}{2}z^2\left[\left(\frac{\partial \theta_x}{\partial x}\right)^2+\left(\frac{\partial \theta_y}{\partial x}\right)^2\right]$$

$$\varepsilon_{ynl}=\frac{1}{2}\left(\frac{\partial u}{\partial y}\right)^2+\frac{1}{2}\left(\frac{\partial v}{\partial y}\right)^2+\frac{1}{2}\left(\frac{\partial w}{\partial y}-\frac{v}{R_y}\right)^2+\frac{1}{2}z^2\left[\left(\frac{\partial \theta_x}{\partial y}\right)^2+\left(\frac{\partial \theta_y}{\partial y}\right)^2\right] \tag{5}$$

$$\gamma_{xynl}=\frac{\partial u}{\partial x}\left(\frac{\partial u}{\partial y}\right)+\frac{\partial v}{\partial x}\left(\frac{\partial v}{\partial y}\right)+\left(\frac{\partial w}{\partial x}\right)\left(\frac{\partial w}{\partial y}-\frac{v}{R_y}\right)+z^2\left[\left(\frac{\partial \theta_x}{\partial x}\right)\left(\frac{\partial \theta_x}{\partial y}\right)+\left(\frac{\partial \theta_y}{\partial x}\right)\left(\frac{\partial \theta_y}{\partial y}\right)\right]$$

The constant R_y identify the radius of curvature in the y directions. C_1 and C_2 are tracers by which the analysis can be reduced to that of Sander's, Love's and Donnell's theories. If $C_1 = C_2 = 1$, the equation corresponds to Sander's theory. For the case $C_1 = 1$, $C_2 = 0$ the equation reduces to Love's theory. For $C_1 = C_2 = 0$, the equation reduced to shear deformable version of Donnell's theory. u, v, w are the displacement in x, y and z directions respectively, θ_x and θ_y are the rotations of the cross section perpendicular to y and x axes respectively.

2.2 Constitutive relations

The constitutive relations for the cylindrical shell panel subjected to temperature and moisture used in the present buckling analysis are in line with Biswal *et al*. (2015).

$$\{F\}=[D]\{\varepsilon\}-\{F^N\} \tag{6}$$

Where

$$\{F\}=\{N_x,N_y,N_{xy},M_x,M_y,M_{xy},Q_x,Q_y\}^T \tag{7}$$

$$\{F^N\}=\{N_x^N,N_y^N,N_{xy}^N,M_x^N,M_y^N,M_{xy}^N,0,0\}^T \tag{8}$$

$$\{\varepsilon\}=\{\varepsilon_x,\varepsilon_y,\gamma_{xy},\kappa_x,\kappa_y,\kappa_{xy},\phi_x,\phi_y\}^T \tag{9}$$

Where $\{F^N\}$ is the non- mechanical force due to hygrothermal loads.

2.3 Finite element analysis

An eight-noded isoparametric element with five degrees of freedom (u, v, w, θ_x and θ_y) at each node is used for the present buckling analysis of woven fiber composite shells subjected to hygrothermal loading. The elastic stiffness matrix, stress stiffness matrix due to hygrothermal conditions, geometric stiffness matrix due to applied in-plane loads and the nodal load vector of the element are evaluated by using the the principle of minimum potential energy (Cook *et al*. 2007).

2.3.1 Element elastic stiffness matrix

The element elastic stiffness matrix is given by

$$[K_e] = \int\int [B]^T [D][B] dxdy \tag{10}$$

where [*B*] is strain displacement matrix and [*D*] is stress-strain matrix.

2.3.2 Element stress stiffness matrix due to hygrothermal loads

The element residual stress stiffness matrix due to hygrothermal loading is given by

$$[K^r_{\sigma e}] = \int\int [G]^T [S][G] dxdy \tag{11}$$

$$[G] = \sum_{i=1}^{8} \begin{bmatrix} \frac{\partial N_i}{\partial x} & 0 & 0 & 0 & 0 \\ \frac{\partial N_i}{\partial y} & 0 & 0 & 0 & 0 \\ 0 & \frac{\partial N_i}{\partial x} & 0 & 0 & 0 \\ 0 & \frac{\partial N_i}{\partial y} & \frac{N_i}{R_y} & 0 & 0 \\ 0 & 0 & \frac{\partial N_i}{\partial x} & 0 & 0 \\ 0 & -\frac{N_i}{R_y} & \frac{\partial N_i}{\partial y} & 0 & 0 \\ 0 & 0 & 0 & \frac{\partial N_i}{\partial x} & 0 \\ 0 & 0 & 0 & \frac{\partial N_i}{\partial y} & 0 \\ 0 & 0 & 0 & 0 & \frac{\partial N_i}{\partial x} \\ 0 & 0 & 0 & 0 & \frac{\partial N_i}{\partial y} \\ 0 & 0 & 0 & N_i & 0 \\ 0 & 0 & 0 & 0 & N_i \end{bmatrix}$$

$$[S]=\begin{bmatrix}
N_x^N & & & & & & & & & & \\
N_{xy}^N & N_y^N & & & & & & & & & \\
0 & 0 & N_x^N & & & & & & & & \\
0 & 0 & N_{xy}^N & N_y^N & & & & sym & & & \\
0 & 0 & 0 & 0 & N_x^N & & & & & & \\
0 & 0 & 0 & 0 & N_{xy}^N & N_y^N & & & & & \\
0 & 0 & -M_x^N & -M_{xy}^N & 0 & 0 & \dfrac{N_x^N h^2}{12} & & & & \\
0 & 0 & -M_{xy}^N & -M_y^N & 0 & 0 & \dfrac{N_{xy}^N h^2}{12} & \dfrac{N_y^N h^2}{12} & & & \\
M_x^N & M_{xy}^N & 0 & 0 & 0 & 0 & 0 & 0 & \dfrac{N_x^N h^2}{12} & & \\
M_{xy}^N & M_y^N & 0 & 0 & 0 & 0 & 0 & 0 & \dfrac{N_{xy}^N h^2}{12} & \dfrac{N_y^N h^2}{12} & \\
0 & 0 & 0 & 0 & 0 & 0 & 0 & 0 & 0 & 0 & 0 \\
0 & 0 & 0 & 0 & 0 & 0 & 0 & 0 & 0 & 0 & 0\ 0
\end{bmatrix}$$

2.3.3 Element geometric stiffness matrix due to applied in-plane load

The geometric stiffness matrix due to applied in-plane loading is expressed as

$$[K_{\sigma e}^a]=\int\int[H]^T[P][H]dxdy \tag{12}$$

2.3.4 Element load vector

The element load vector due to hygrothermal forces and moments is given by

$$\{P_e^N\}=\int\int[B]^T\{F^N\}dxdy \tag{13}$$

2.4 Solution process

The element matrices are assembled to obtain the respective global matrices [K], the elastic stiffness matrix; [K_σ^r], the initial stress stiffness matrix due to hygrothermal condition; [K_σ^a], the geometric stiffness matrix due to applied in-plane load. Based on the degree of polynomial involves in the displacement function the full (3×3) numerical integration is usually required, but this may introduced shear locking problem in the 8-noded finite element. To avoid possible shear locking, the order of integration is reduced by employing reduced integral procedure (Ferreira and Barbosa 2000). (2×2) reduced numerical integration by Gaussian quadrature is employed for the computation of stiffness matrices. Finally linear buckling loads are determined from the following condition

$$\left|[[K]+[K_\sigma^r]]-P_{cr}\left[K_\sigma^a\right]\right|=0 \tag{14}$$

P_{cr} is the buckling load. Eq. (14) is a generalized eigenvalue problem and is solved using MATLAB.

3. Experimental study

The cylindrical composite shell panels of three different radius of curvatures (R=0.867m, 1.154 m and 2.09 m) used in the present experimental study were prepared using three prefabricated cylindrical moulds of corresponding curvatures as shown in Fig. 3. The shell panel specimens were fabricated by hand layup method using woven roving glass fibers (WR 360/100, Owens Corning– 360 g/m^2) with epoxy as matrix. The weight fraction of fiber to matrix was 50:50. Hardener (Ciba-Geigy, Araldite HY556 and Hardener HY951) 8% of the weight of epoxy was used for preparation of epoxy resin matrix. Fabrication was done with the application of a gel coat (Epoxy and Hardener) deposited on the mould and glass fiber sheets. After proper curing of laminates, the specimens were cut into 250 mm × 25 mm size for tensile test and 210 mm × 210 mm size for buckling testing. The average thicknesses of 16, 12 and 8 layered laminate was measured by digital slide callipers and found to be 6 mm, 4.5 mm and 3 mm respectively.

3.1 Hygrothermal conditioning

The fabricated laminated composite cylindrical curved panels and the tensile test specimens were hygrothermally conditioned in oven (Fig. 4) and humidity chamber (Fig. 5) separately before testing. For temperature effects all the specimens were kept in oven at temperature of 315K, 330K, 345 K and 360 K for a period of 8 to 10 hours. For effects of moisture concentrations the specimens were kept in humidity chamber as per ASTM-D5229-04 (2004) for 0.1%, 0.2%, 0.3% and 0.4% moisture concentration. The moisture concentration was determined by using Eq. (15) as per ASTM-D5229-04 (2004).

$$M\% = \left[\frac{W_i - W_0}{W_0}\right] \times 100 \tag{15}$$

W_i is current moist weight and W_0 is oven-dried weight of specimen in g, respectively.

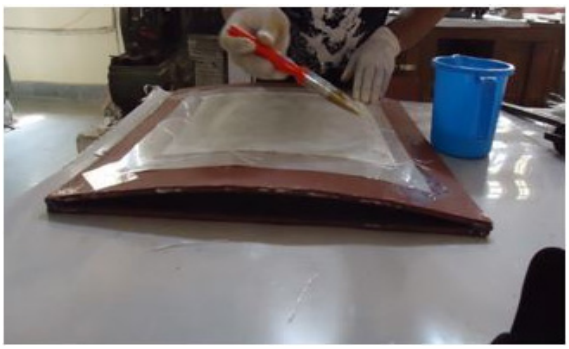

Fig. 3 Fabrication of laminated cylindrical shell panel

Fig. 4 Composite shell panels in oven

Fig. 5 Composite shell panels in humidity chamber

Table 1 Elastic moduli of woven fabric Glass/Epoxy lamina at different temperatures, $\alpha_1 = -0.3 \times 10^{-6}$/K, $\alpha_2 = 28.1 \times 10^{-6}$/K, $\upsilon_{12} = 0.41$, $G_{12} = G_{13} = G_{23}$, $E_1 = E_2$, $\rho = 1690$ kg/m^3

Elastic moduli	Temperature, T_E (K)				
	300	315	330	345	360
E_1 (GPa)	15.94	15.79	15.69	15.48	14.16
G_{12} (GPa)	3.57	3.57	3.54	3.53	3.50

Table 2 Elastic moduli of woven fabric Glass/Epoxy lamina at different moisture concentration, $\beta_1 = 0$, $\beta_2 = 0.44$, $\upsilon_{12} = 0.41$, $G_{12} = G_{13} = G_{23}$, $E_1 = E_2$, $\rho = 1690$ kg/m^3

Elastic moduli	Moisture concentration, C (%)				
	0	0.1	0.2	0.3	0.4
E_1 (GPa)	15.94	15.76	15.73	15.64	15.34
G_{12} (GPa)	3.57	3.53	3.53	3.47	3.47

3.2 Determination of material constants

Unidirectional tensile tests were done on hygrothermally treated tensile specimens in universal testing machine (INSTRON 8862) as described in ASTM-3039/D 3039M-08 (2008) to find the material constants for different temperature and moisture concentrations. The change in elastic moduli of the material with change of temperatures and moisture concentrations are given in Tables 1 and 2 respectively.

3.3 Buckling test

The hygrothermally treated laminated composite cylindrical shell panels ($a = b = 0.21$ m, $R_x = \infty$, $R_y = R$, $\rho = 1690$ kg/m^3) were tested in universal testing machine INSTRON 8862 to determine the critical buckling load as shown in Fig. 6. The CFCF (two vertical faces free, top and bottom

Fig. 6 Buckling test of CFCF laminated cylindrical shell panel on INSTRON 8862

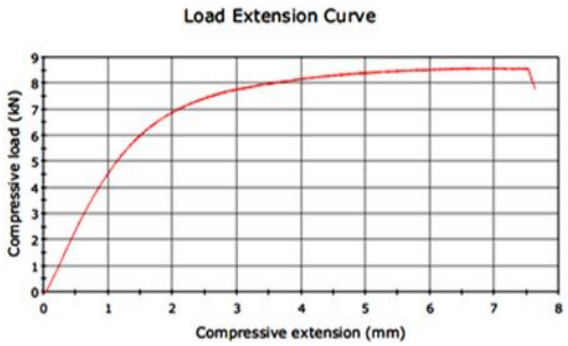

Fig. 7 Load extension curve of CFCF laminated cylindrical shell panel on INSTRON 8862

face clamped) boundary condition is used in the present experimental study. A typical load extension curve of the cylindrical shell with curvature ratio (R_y/b = 4.13) at 0.3% moisture concentration is shown in Fig. 7. To obtain accurate experimental data, three specimens for each type according to curvature, ply orientation and aspect ratio were tested and the average value is considered.

4. Results and discussions

The results on buckling of laminated composite shells subjected to hygrothermal field are considered here. The results are presented in the following sections:

- Convergence studies.
- Comparison with previous studies.
- New examples

4.1 Convergence studies

The convergence studies are carried out for the buckling of woven fiber glass/epoxy laminated composite cylindrical shell panels in thermal environment as shown in Table 3. A mesh of 10×10

Table 3 Convergence of buckling loads (kN) of square simply supported cylindrical shell panels at T_E = 330 K with $[0/90]_{4s}$ lamination for different curvature ratio (R_y/b)

Mesh size	R_y/b			
	4.13	5.49	9.95	∞
4 × 4	45.677	39.266	20.669	13.751
6 × 6	45.181	39.184	20.618	13.708
8 × 8	45.118	39.172	20.612	13.704
10 × 10	45.115	39.17	20.611	13.703

shows good convergence of the numerical solutions for the buckling of laminated cylindrical composite shell panels in hygrothermal field.

4.2 Comparison with previous studies

As part of the validation of the present method, the non-dimensional buckling load obtained from the present formulation for $[0/ -\theta/ \theta/ -90]_s$ cylindrical panels with four edges simply supported subjected to axial compression are compared in Table 4 with the HSDT and classical laminated theory (CPT) solutions of Moita *et al*. (1999) and FSDT solutions of Thinch and Ngoc (2005), using their material and geometrical properties: E_1 = 181 Gpa, E_2 = 10.3 GPa, $G_{12} = G_{13} = G_{23}$ = 7.17 GPa, $v_{12} = v_{13} = v_{23}$ = 0.28, h = 1.0 mm, R/h = 150, a/R = 1.0, b/L = 1.309 and 1.047. A good agreement can be observed between the present FEM based on FSDT and the HSDT solutions of Moita *et al*. (1999). The accuracy and reliability of the formulation are also tested for non-dimensional buckling of [0/90/90/0] laminated composite flat panels with four edges simply supported exposed to hygrothermal field with FEM results of Sairam and Sinha (1992), Whitney and Ashton (1971) and Patel *et al*. (2002) in Table 5. The geometrical and material properties adopted here are: a/b = 1, a/h = 100, E_1 = 130 GPa, E_2 = 9.5 GPa, G_{12} = 6.0 GPa, υ_{12} = 0.3, $G_{13} = G_{12}$, $G_{23} = 0.5\,G_{12}$, $\alpha_1 = -0.3 \times 10^{-6}$/K, $\alpha_2 = 28.1 \times 10^{-6}$/K, $\beta_1 = 0$, $\beta_2 = 0.44$. The above studies indicate good agreement between the present study and those from the literature.

4.3 New results

Numerical results using present FEM formulation and experimental (Exp) results of buckling for woven fiber glass/epoxy composite cylindrical shell panels subjected to uniform distribution of temperature and moisture are obtained for two opposite sides clamped and other two side free (CFCF) boundary condition. The lamina material properties at the elevated temperature and moisture concentration used in the present investigation are presented in Tables 1 and 2 respectively. For all the investigations, unless otherwise mentioned, the geometric properties are taken as: $a = b$ = 0.21 m. The average thickness of the laminate shells measured by digital slide calliper are 3 mm, 4.5 mm and 6 mm for eight layers, twelve layers and sixteen layers laminated cylindrical shell panels respectively.

4.3.1 Effect of curvature on buckling load of cylindrical curved panels in hygrothermal environment

The effect of curvature on buckling load of sixteen layer $[0/90]_{4s}$ woven fiber glass/epoxy composite cylindrical shell panels subjected to different temperature and moisture concentration

Table 4 Comparison of non-dimensional buckling loads $\lambda = P_{cr}R/E_1h^2$ for $[0/ -\theta/ \theta/ -90]_s$ laminated simply supported cylindrical panel (E_1 = 181 Gpa, E_2 = 10.3 GPa, $G_{12} = G_{13} = G_{23}$ = 7.17 GPa, $v_{12} = v_{13} = v_{23}$ = 0.28, h = 1.0 mm, R/h = 150, a/R = 1.0, b/a = 1.309 and 1.047, T_E = 300K, C = 0%)

	b/a = 1.309				b/a = 1.047			
$\theta°$	Present FEM	CPT Moita *et al*. (1999)	HSDT Moita *et al*. (1999)	FSDT Thinch and Ngoc (2005)	Present FEM	CPT Moita *et al*. (1999)	HSDT Moita *et al*. (1999)	FSDT Thinch and Ngoc (2005)
0	0.126	0.117	0.121	0.118	0.112	0.123	0.122	0.119
15	0.156	0.147	0.147	0.149	0.136	0.147	0.147	0.151
30	0.202	0.197	0.190	0.187	0.169	0.194	0.192	0.188
45	0.207	0.221	0.211	0.215	0.197	0.222	0.220	0.217
60	0.199	0.212	0.206	0.208	0227	0.214	0.214	0.212
75	0.184	0.171	0.174	0.175	0.187	0.174	0.179	0.177
90	0.166	0.142	0.147	0.151	0.148	0.144	0.115	0.155

Table 5 Comparison of non-dimensional buckling loads $\lambda = P_{cr}/(P_{cr})_{C=0\% \text{ or } T=300K}$ for simply supported [0/90/90/0] laminated flat panels at 325K temperature and 0.1% moisture concentrations (a/b = 1, a/h = 100, E_1 = 130 Gpa, E_2 = 9.5 Gpa, G_{12} = 6.0 Gpa, v_{12} = 0.3, $G_{13} = G_{12}$, G_{23} = 0.5 G_{12})

Source	Temperature (K)	Moisture concentrations (%)
	T = 325 K	C = 0.1%
Present FEM	0.4481	0.6095
Sairam and Sinha (1992)	0.4488	0.6099
Whitney and Ashton (1971)	0.4477	0.6091
Patel *et al*. (2002)	0.4466	0.6084

are presented both numerically (FEM) and experimentally (Exp) in Figs. 8 and 9 respectively. For laminated square composite cylindrical shells the buckling load is presented numerically as well as experimentally for four different curvature ratios ($R_y/b = R/b$ = 4.13, 5.49, 9.95 and ∞) under CFCF boundary conditions.

Fig. 8 shows the FEM and experimental result for buckling load of $[0/90]_{4s}$ glass/epoxy woven fiber cylindrical curved panels for four different curvature ratios with uniformly variation of temperature under CFCF boundary condition. It is observed from Fig. 8, that the buckling load increases with increasing the curvature from plate to shell due to increasing of stiffness. Here it is observed that the critical load capacity of CFCF panels reduce significantly and become much less with increase of temperature. With increasing the temperature from 300 K to 345 K the buckling load decreases by 70.63%, 76.61%, 82.94% and 85.91% for cylindrical shells with curvature ratio 4.13, 5.49, 9.95 and ∞ (plate) respectively, due to the reduction of the stiffness of the shell in thermal environment. At reference temperature (300 K) the buckling load increases by 22.37%, 13.06% and 4.2% by changing the curvature ratio from ∞ (plate) to curvature ratio 4.13, 5.49 and 9.95 respectively. It can observe that there is a good agreement between FEM result and buckling test result.

The critical load obtained from present FEM and buckling test (Exp) results at different

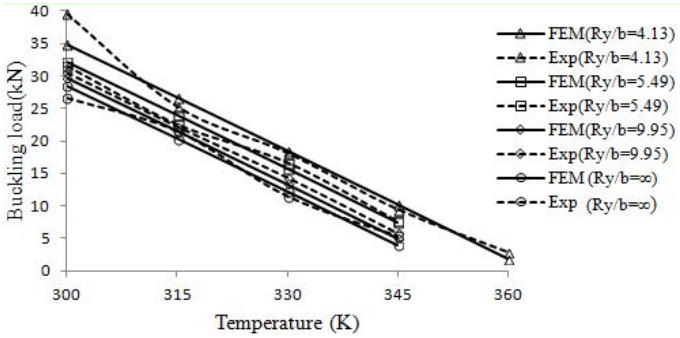

Fig. 8 Effects of temperature on buckling load of $[0/90]_{4s}$ CFCF cylindrical curved panels

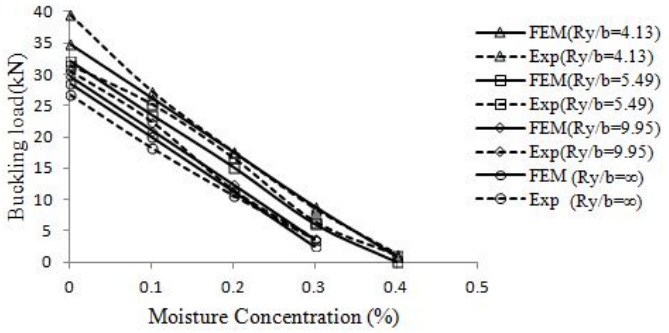

Fig. 9 Effects of moisture on buckling load of $[0/90]_{4s}$ CFCF cylindrical curved panels

moisture concentrations for sixteen layered $[0/90]_{4s}$ glass/epoxy cylindrical shell panels with CFCF boundary condition for different curvature ratios are investigated in Fig. 9. The results shows that the buckling load suffer in a range of 74.6%, 80.9%, 87.63%, and 90.8% decrease with increasing the moisture concentrations from 0 to 0.3% for cylindrical shells with curvature ratios 4.13, 5.49, 9.95 and ∞ (plate) respectively. The buckling loads of cylindrical shells in moist environment are greatly affected with CFCF boundary condition due to the extreme reduction of the stiffness of the shells at elevated moisture concentrations.

4.3.2 Effect of ply orientation on buckling load of cylindrical curved panels in hygrothermal environment

The study is further extended for the buckling of laminated cylindrical shell with curvature ratio (R_y/b = 4.13) for different lamination sequence in hygrothermal environment both numerically (FEM) and experimentally (Exp). Three different lamination sequence $[0/90]_{4s}$, $[45/-45]_{4s}$ and $[30/-30]_{4s}$ are considered here. Results for the variation of buckling load of sixteen layer symmetric cross-ply$[0/90]_{4s}$ and sixteen layer symmetric angle-ply $[45/-45]_{4s}$ woven fiber glass/ epoxy composite cylindrical shell subjected to different temperature and moisture concentration under CFCF boundary condition are presented in Figs. 10 and 11 respectively.

As shown in Fig. 10, the buckling load of woven fabric laminated composite cylindrical shells is least affected by changing the lamination sequence from $[0/90]_{4s}$ to $[45/-45]_{4s}$ lamination. With increasing the temperature from 300 K to 345 K the buckling load is decreasing by 70.63% and 72.5% for $[0/90]_{4s}$ and $[45/-45]_{4s}$ cylindrical shell respectively.

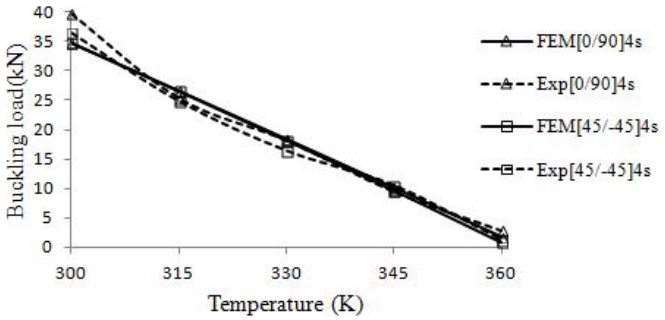

Fig. 10 Effects of temperature on buckling load of CFCF cylindrical shell panels (R_y/b=4.13)

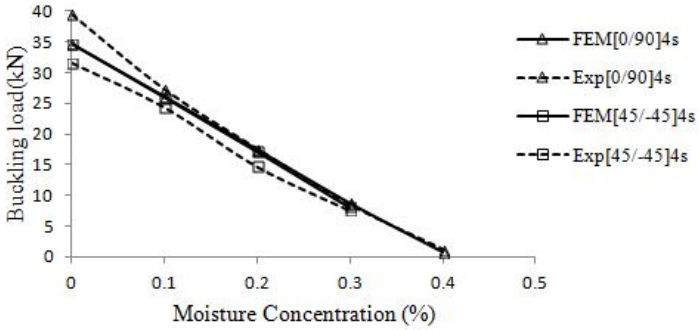

Fig. 11 Effects of moisture on buckling load of CFCF cylindrical shell panels (R_y/b = 4.13)

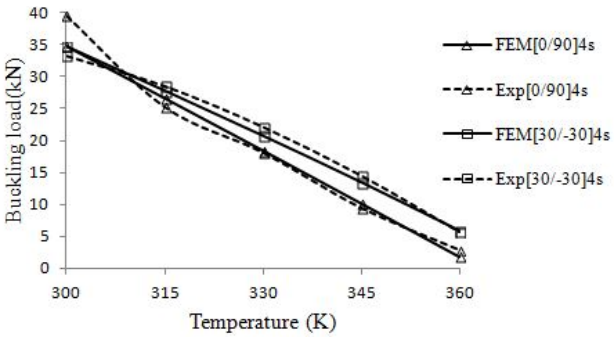

Fig. 12 Effects of temperature on buckling load of CFCF cylindrical shell panels (R_y/b = 4.13)

Fig. 11 shows that, the buckling load is reducing in the range of 74.6% and 76.6% for $[0/90]_{4s}$ and $[45/-45]_{4s}$ cylindrical shell respectively as the moisture concentration raised from 0 to 0.3% due to reduction of stiffness in moist environment.

Effects of temperature on critical load of $[0/90]_{4s}$ and $[30/-30]_{4s}$ woven fiber glass/epoxy composite cylindrical shell under CFCF boundary condition are presented in Fig. 12. As observed in Fig. 12, the buckling load of woven fabric laminated composite cylindrical shells at elevated temperature is increasing slightly by changing the lamination sequence from $[0/90]_{4s}$ to $[30/-30]_{4s}$ lamination. The buckling load is decreasing by 94.68% and 83.26% with increasing the temperature from 300 K to

360 K for $[0/90]_{4s}$ and $[30/-30]_{4s}$ cylindrical shell panels respectively.

Fig. 13 shows, the effects of moisture concentration on buckling load of $[0/90]_{4s}$ and $[30/-30]_{4s}$ woven fiber glass/epoxy composite cylindrical shell under CFCF boundary condition. It is found that the buckling load is reducing by 97.5% and 88.6% with increasing the moisture concentration from 0 to 0.4% for $[0/90]_{4s}$ and $[30/-30]_{4s}$ cylindrical shell panels respectively.

4.3.3 Effect of aspect ratio on buckling load of cylindrical curved panels in hygrothermal environment

The effects of uniform temperature on critical load of sixteen layer symmetric cross-ply $[0/90]_{4s}$ cylindrical curved panels with curvature ratio (R_y/b = 4.13) in CFCF boundary condition for aspect ratios 0.25, 0.5 and 1.0 is shown in Fig. 14 both numerically and experimentally. It is found that the critical load of the curved panels increases with increasing the aspect ratio. There is a greater reduction in critical loads when temperature exceeds 330 K for curved panel with aspect ratio 0.25 due to residual stress developed in thermal field. Similar effects were also observed by Sairam and Sinha (1992) for the laminated composite plates.

The numerical and experimental results for buckling load of $[0/90]_{4s}$ laminated cylindrical shell panels with curvature ratio (R_y/b = 4.13) under CFCF boundary condition are given in Fig. 15 against moisture for three different aspect ratios. It is noticed that the buckling load of the shell with aspect ratio 0.25 approaches to zero beyond 0.3% moisture concentrations due to the extreme reduction of the stiffness of the shells at elevated moisture concentration.

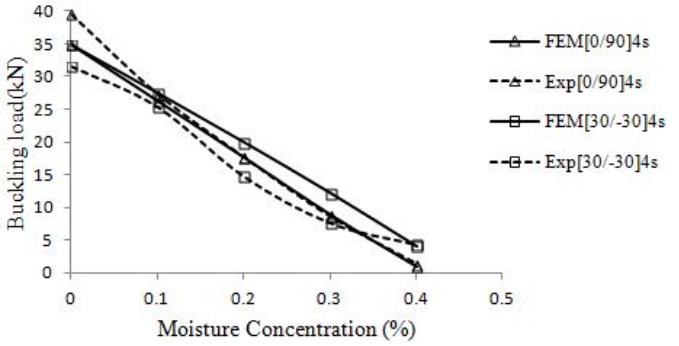

Fig. 13 Effects of moisture on buckling load of CFCF cylindrical shell panels (R_y/b = 4.13)

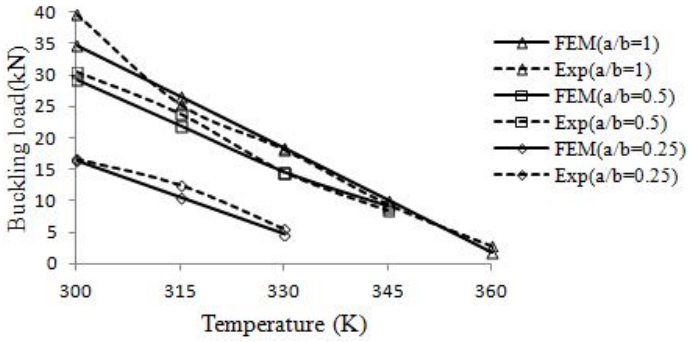

Fig. 14 Effects of temperature on buckling load of CFCF cylindrical shell panels (R_y/b = 4.13)

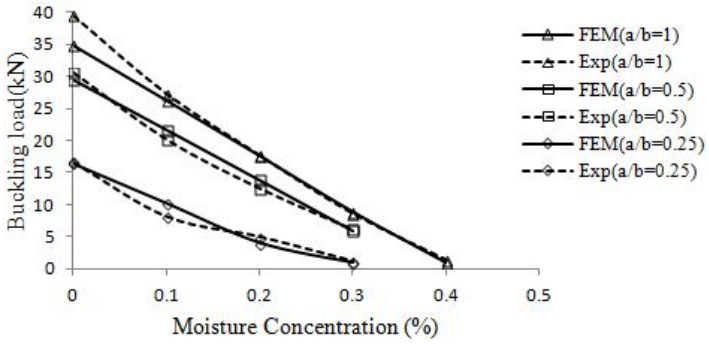

Fig. 15 Effects of moisture on buckling load of CFCF cylindrical shell panels (R_y/b = 4.13)

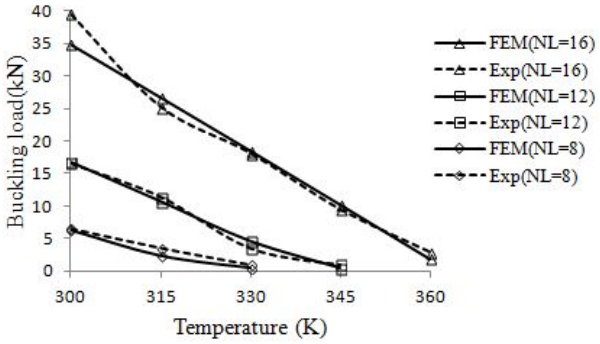

Fig. 16 Effects of temperature on buckling load of CFCF cylindrical shell panels (R_y/b = 4.13)

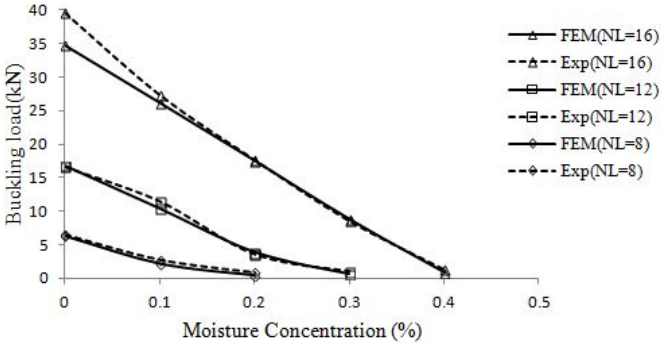

Fig. 17 Effects of moisture on buckling load of CFCF cylindrical shell panels (R_y/b = 4.13)

4.3.4 Effect of number of layers on buckling load of cylindrical curved panels in hygrothermal environment

The variation of buckling load of woven fiber glass/epoxy composite cylindrical shell with curvature ratio (Ry/b = 4.13) subjected to different temperature and moisture concentration for different number of layers of laminate are computed numerically by the present finite element formulation and compared with the buckling test result in Figs. 16-17 for CFCF boundary condition. Results are presented for symmetric cross-ply cylindrical shells with eight, twelve and

sixteen layer laminates ($[0/90]_{2s}$, $[0/90]_{3s}$ and $[0/90]_{4s}$).

Under CFCF boundary condition the buckling load is reduced in the range of 70.63% for 16 layers cylindrical shells by the increment of temperature from 300 K to 345 K, but 12 layers and 8 layers cylindrical shell become unstable at 345 K and 330 K temperature respectively as seen in Fig. 16 because of reduction of stiffness of the cylindrical shell in thermal environment.

From Fig. 17 it is observed that, the buckling load approaches to zero at 0.2%, 0.3% and 0.4% moisture concentration for 8 layer, 12 layer and 16 layer shells respectively due to the extreme reduction of the stiffness of the shells at elevated moisture concentrations.

5. Conclusions

In order to assess the effects of temperature and moisture concentration on the buckling behaviour of laminated composite shell panels a computer code is developed in MATLAB environment with generalised FEM formulation. A number of experiments are conducted for cylindrical shell panels with different curvature ratios, lamination sequence, number of layers and aspect ratios subjected to uniform change of temperature and moisture concentrations for comparison with FEM results. The broad conclusions made from the above investigation are given below:

- There is a good agreement between the FEM and buckling test results.
- The buckling load of cylindrical curved panels increases with decreasing the curvature ratios.
- The buckling load of laminated composite shells reduces with increase in temperature and moisture concentration due to reduction of the stiffness.
- The buckling load of woven fiber laminated composite cylindrical shell is least affected by the lamination sequences.
- With increasing the number of layers of laminates the buckling load of laminated composite shells increases.
- The cylindrical shell panels become unstable at higher temperature and moisture concentration depending upon the curvature, number of layers of laminate and aspect ratio.

Benchmark experimental results on buckling of composite shell panels are presented in this study for reference of future researchers. The buckling load of laminated composite shell panels are significantly affected by the temperature and moisture conditions along with the geometry of the panels. The buckling results presented in this investigation can be used as design aids for laminated composite shell panels subjected to hygrothermal loading along with in-plane stress for the range of geometry and material parameters considered in this study.

References

Agency, E.S. (2012), SA Studies future of Europe's launches services; 25 July 2012.

ASTM Standard: D5229/D5229M-04 (2004), Standard test method for moisture absorption.

ASTM Standard: D3039/D3039M-08 (2008), Standard test method for tensile properties of polymer matrix composite materials.

Belabed, Z., Houari, M.S.A., Tounsi, A., Mahmoud, S.R. and Bég, O.A. (2014), "An efficient and simple higher order shear and normal deformation theory for functionally graded material (FGM) plates", *Composites*: *Part B*, **60**, 274-283.

Bellifa, H., Benrahou, K.H., Hadji, L., Houari, M.S.A. and Tounsi, A. (2016), "Bending and free vibration analysis of functionally graded plates using a simple shear deformation theory and the concept the neutral surface position", *J. Brazil. Soc. Mech. Sci. Eng.*, **38**(1), 265-275.

Bennoun, M., Houari, M.S.A. and Tounsi, A. (2016), "A novel five variable refined plate theory for vibration analysis of functionally graded sandwich plates", *Mech. Adv. Mater. Struct.*, **23**(4), 423-431.

Bert, C.W. and Birman, V. (1987), "Dynamic instability of shear deformable antisymmetric angle-ply plates", *Int. J. Solid. Struct.*, **23**(7), 1053-1061.

Biswal, M., Sahu, S.K. and Asha, A.V. (2015), "Experimental and numerical studies on free vibration of laminated composite shallow shells in hygrothermal environment", *Compos. Struct.*, **127**,165-174.

Bouderba, B., Houari, M.S.A. and Tounsi, A. (2013), "Thermomechanical bending response of FGM thick plates resting on Winkler–Pasternak elastic foundations", *Steel Compos. Struct., Int. J.*, **14**(1), 85-104.

Bouderba, B., Houari, M.S.A., Tounsi, A. and Mahmoud, S.R. (2016), "Thermal stability of functionally graded sandwich plates using a simple shear deformation theory", *Struct. Eng. Mech., Int. J.*, **58**(3), 397-422.

Bourada, M., Kaci, A., Houari, M.S.A. and Tounsi, A. (2015), "A new simple shear and normal deformations theory for functionally graded beams", *Steel Compos. Struct., Int. J.*, **18**(2), 409-423.

Bouguenina, O., Belakhdar, K., Tounsi, A. and Bedia, E.A.A. (2015), "Numerical analysis of FGM plates with variable thickness subjected to thermal buckling", *Steel Compos. Struct., Int. J.*, **19**(3), 679-695.

Carrera, E. (1988), "The effects of shear deformation and curvature on buckling and vibrations of cross-ply laminated composite doubly curved shells", *J. Sound Vib.*, **150**(3), 405-433.

Cook, R.D., Malkus, D.S., Plesha, M.E. and Witt, R.J. (2007), *Concepts and Applications of Finite Element Analysis*, (4th Edition), John Wiley and Sons, Singapore.

Ferreira, A.J.M. and Barbosa, J.T. (2000), "Buckling behaviour of composite shells", *Compos. Struct.*, **50**(1), 93-98.

Hamidi, A., Houari, M.S.A., Mahmoud, S.R. and Tounsi, A. (2015), "A sinusoidal plate theory with 5-unknowns and stretching effect for thermomechanical bending of functionally graded sandwich plates", *Steel Compos. Struct., Int. J.*, **18**(1), 235-253.

Hebali, H., Tounsi, A., Houari, M.S.A., Bessaim, A. and Bedia, E.A.A. (2014), "A new quasi-3D hyperbolic shear deformation theory for the static and free vibration analysis of functionally graded plates", *ASCE J. Eng. Mech.*, **140**(2), 374-383.

Hsu, Y.S., Reddy, J.N. and Bert, C.W. (1981), "Thermoelasticity of circular cylindrical shells laminated of bimodulus composite materials", *J. Therm. Stress.*, **4**(2), 155-177.

Jun, S.M. and Hong, C.S. (1988), "Buckling behavior of laminated composite cylindrical panels under axial compression", *Comput. Struct.*, **29**(3),479-490.

Jung, W.Y. and Han, S.C. (2014), "Shear buckling responses of laminated composite shells using a modified 8-node ANS shell element", *Compos. Struct.*, **109**, 119-129.

Kar, V.R., Mahapatra T.R. and Panda, S.K. (2015), "Nonlinear flexural analysis of laminated composite flat panel under hygro-thermo-mechanical loading", *Steel Compos. Struct., Int. J.*, **19**(4), 1011-1033.

Khdeir, A.A., Reddy, J.N. and Frederick, D. (1989), "A study of bending, vibration and buckling of cross-ply circular cylindrical shells with various shell theories", *Int. J. Eng. Sci.*, **27**(11), 1337-1351.

Kim, K.D. (1996), "Buckling behaviour of composite panels using the finite element method", *Compos. Struct.*, **36**(1-2), 33-43.

Kundu, C.K. and Sinha, P.K. (2007), "Post-buckling analysis of laminated composite shells", *Compos. Struct.*, **78**(3), 316-324.

Lal, A., Singh, B.N. and Kale, S. (2011), "Stochastic post buckling analysis of laminated composite cylindrical shell panel subjected to hygrothermomechanical loading", *Compos. Struct.*, **93**(4), 1187-1200.

Lee, S.Y. and Yen, W.J. (1989), "Hygrothermal effects on the stability of a cylindrical composite shell panel", *Comput. Struct.*, **33**(2), 551-559.

Li, Z.M. and Qiao, P. (2015), "Buckling and postbuckling of anisotropic laminated cylindrical shells under combined external pressure and axial compression in thermal environments", *Compos. Struct.*, **119**, 709-726.

Mahi, A., Bedia, E.A.A. and Tounsi, A. (2015), "A new hyperbolic shear deformation theory for bending and free vibration analysis of isotropic, functionally graded, sandwich and laminated composite plates", *Appl. Math. Model.*, **39**(9), 2489-2508.

Matsunaga, H. (1999), "Vibration and stability of thick simply supported shallow shells subjected to in-plane stresses", *J. Sound Vib.*, **225**(1), 41-60.

Meziane M.A.A., Abdelaziz, H.H. and Tounsi, A. (2014), "An efficient and simple refined theory for buckling and free vibration of exponentially graded sandwich plates under various boundary conditions", *J. Sandw. Struct. Mater.*, **16**(3), 293-318.

Moita, J.S., Mota Soares, C.M. and Mota Soares, C.A. (1999), "Buckling and dynamic behaviour of laminated composite structures using a discrete higher-order displacement model", *Comput. Struct.*, **73**(1-5), 407- 423.

Nosier, A. and Reddy, J.N. (1992), "Vibration and stability analyses of cross-ply laminated circular cylindrical shells", *J. Sound Vib.*, **157**(l), 139-159.

Patel, B.P., Ganapathi, M. and Makhecha, D.P. (2002), "Hygrothermal effects on the structural behaviour of thick composite laminates using higher-order theory", *Compos. Struct.*, **56**(1), 25-34.

Rajanna, T., Banerjee, S., Desai, Y.M. and Prabhakara, D.L. (2016), "Vibration and buckling analyses of laminated panels with and without cutouts under compressive and tensile edge loads", *Steel Compos. Struct.*, *Int. J.*, **21**(1), 37-55.

Reddy, J.N. (1984), "Exact solutions of moderately thick laminated shells", *J. Eng. Mech.*, **110**(5), 794-809.

Ren, M., Li, T., Huang, Q. and Wang, B. (2014), "Numerical investigation into the buckling behavior of advanced grid stiffened composite cylindrical shell", *J. Reinf. Plast. Compos.*, **33**(16), 1508-1519.

Sairam, K.S. and Sinha, P.K. (1992), "Hygrothermal effects on the buckling of laminated composite plates", *Compos. Struct.*, **21**(4), 233-247.

Sairam, K.S. and Babu, T.S. (2002), "Buckling of laminate composite shells under transverse load", *Compos. Struct.*, **55**(2),157-168.

Shen, S.H. (2000), "Hygrothermal effects on the post-buckling of composite laminated cylindrical shells", *Compos. Sci. Technol.*, **60**(8), 1227-1240.

Sheng, G.G. and Wang, X. (2008), "Thermal vibration, buckling and dynamic stability of functionally graded cylindrical shells embedded in an elastic medium", *J. Reinf. Plast. Compos.*, **27**(2), 117-134.

Simitses, G.J. (1996), "Buckling of moderately thick laminated cylindrical shells: A review", *Compos. Part B*, **27**(6), 581-587.

Singh, B.N. and Babu, J.B. (2009), "Thermal buckling of laminated conical shells embedded with and without piezoelectric layer", *J. Reinf. Plast. Compos.*, **28**(7), 791-812.

Thangaratnam, R.K., Palaninathan, R. and Ramachandran, J. (1990), "Thermal buckling of laminated composite shells", *AIAA Journal*, **28**(5), 859-860.

Thinh, T.I. and Ngoc, L.K. (2005), "Buckling analysis of laminated cylindrical composite shell panel under mechanical and hygrothermal loads", *Vietnam J. Mech.*, **27**(1), 1-12.

Tounsi, A., Houari, M.S.A., Benyoucef, S. and Bedia, E.A.A. (2013), "A refined trigonometric shear deformation theory for thermoelastic bending of functionally graded sandwich plates", *Aerosp. Sci. Technol.*, **24**(1), 209-220.

Whitney, J.M. and Ashton, J.E. (1971), "Effect of environment on the elastic response of layered composite plates", *Am. Inst. Aeronaut. Astronaut. J.*, **9**(9), 1708-1713.

Yahia, S.A, Atmane, H.A., Houari, M.S.A. and Tounsi, A. (2015), "Wave propagation in functionally graded plates with porosities using various higher-order shear deformation plate theories", *Struct. Eng. Mech.*, *Int. J.*, **53**(6), 1143-1165.

Zidi, M., Tounsi, A., Houari, M.S.A., Bedia, E.A.A. and Bég, O.A. (2014), "Bending analysis of FGM plates under hygro-thermo-mechanical loading using a four variable refined plate theory", *Aerosp. Sci. Technol.*, **34**, 24-34.

CC